Alfarama Journal of Basic & Applied Sciences

https://ajbas.journals.ekb.eg
ajbas@sci.psu.edu.eg

Faculty of Science Port Said University

http://sci.psu.edu.eg/en/

October 2023, Volume 4 , Issue IV

DOI:**https://doi.org/10.21608/ajbas.2023.187857.1140**

ISSN 2682-275X

Submitted: 23/01/2023
Accepted: 07/06/2023

Pages: 680 - 693

Geoenvironmental hazards assessment in the Northwest Suez Canal region, Egypt

Ahmed Gh. Ahmed Hassan [1,*], Hatem F. Hassan [2], Ahmed E. El-Rayes[3], Mohamed Arnous[4]

[1, 2] Geology Department, Faculty of Science, Port Said University, Port Said 42526, Egypt.

[3, 4] Geology Department, Faculty of Science, Suez Canal University, Ismailia 41522, Egypt.

***Corresponding author:** a.g.a.hassan90@gmail.com

ABSTRACT

Waterlogging and soil salinization is a threat to arid regions around the world. The study area is in the Northwestern Suez Canal Region (NWSCR), with a high population density and significant agricultural activity. Waterlogging, salt-affected soil, and land degradation are among the most common hazards caused by human activity in the NWSCR. In the current work, remote sensing data, and the Global Digital Elevation Model (GDEM) are integrated using Geographic Information System (GIS) techniques to assess the prevalent geo-environmental hazards at the NWSCR. The findings indicate that the NWSCR is extremely vulnerable to water logging and soil salinization, with a strong relation to human activities. The obtained finding indicates that 41.66 km^2 of the NWSCR (4900.02746 Km^2) is permanently water-logged (0.85% percent) is influenced by temporary water-logged areas, and 26.32 km^2(0.53 % percent) is influenced by soil salinization. As a result of flood-irrigation practices, human activity, and arid conditions, the NWSCR has a lot of water-logged zones and salinized soil. This study recommends using modern irrigation systems to avoid waterlogging and soil salinization.

Key Words:

Geo-environmental, Hazards, GIS, Remote Sensing, Geo-spatial mapping, Suez Canal Region

1-INTRODUCTION

Observing change patterns over time is critical for answering questions like "what happened here?" in strategically important places like the Northwest Suez Canal region (NWSCR), where change is an axiom with both positive and negative consequences. Environmental change is caused by both natural and human factors. While human activities may cause pollution and land degradation, natural changes such as coastal erosion and climate change may also occur. Due to its close vicinity to Lake Manzala, the Suez Canal, and the Mediterranean Sea, the Northwest Suez Canal Region (NWSCR) is of utmost significance. Numerous environmental impact hazards, caused by natural and man-made elements such as water logging and soil salinization, and agricultural areas shortage, have been recognized in the NWSCR [1] [2] [3].

Remote sensing (RS) has become necessary for managing natural resources. Every sustainable development plan in the world involves monitoring and evaluating the availability and effectiveness of geo-environmental hazard indicators based on RS, GIS, and Global Positioning Systems (GPS). For surveying, categorizing, mapping, monitoring, characterizing, and tracking changes in composition, extent, spatial distribution, surface changes, and determining and evaluating various LU-LC classes, RS and GIS approaches offer highly effective tools and techniques. The assessment method suggested in the current study aims to establish trends in measurements or conditions, establish rates or levels of various phenomena like waterlogging and salinization, identify the causes of rates and trends, and identify the kind and impact of the consequences of rates and trends. Additionally, mitigation measurements serve as the necessary implementation of rules and instructions. To address the severe geo-environmental hazards, loss of natural resource productivity, and degradation of the land, particularly in dry lands. [4, 5, 6, 7]. RS technologies demonstrated effective methods for identifying and tracking geo-environmental hazards [8, 9, 10]. It is distinguished by fast and low-cost, technology providing high-quality data. Due to its high temporal frequency, computed data (digital format), and high spectral and spatial resolutions, RS tools with data have become a primary source for investigating change detection. Change detection is the process of determining differences in objects by repeating observations at different times [11]. The overall goal of change detection studies in RS is to highlight land cover-land use (LC-LU) on digital images. LC-LU are two distinct expressions, where (LC) refers to physical features that cover the Earth's surface, such as water bodies, vegetation cover, urban areas, and various human activities, and (LU) refers to human activity that is influenced by the physical features of the Earth's surface[1,12]. LU influences LC, but changes in LC caused by LU do not always result in land degradation. In the current work, LC-LU maps for all classes were created for the years 1984, 2000, and 2018. These maps depict the detection of change at the NWSCR over 34-year period.

Numerous experts in their fields have investigated the NWSCR, [3,8,13,14]. These studies gave us information on many sorts of attitudes that must be combined in order to address numerous geological and environmental issues such as land degradation, water resources pollution, hydro-environmental, and geoenvironmental hazards assessment. Several others, from an environmental standpoint, paid more attention to the environmental hazard revealed by the NWSCR[1,15,16]. They stated that the study area was under threat of the same environmental hazards, such as waterlogging [17], soil salinization [1], and coastal erosion [15]. The NWSCR, as a portion of the Nile Delta, has the same lithological composition and is affected by the same tectonic setting. The Suez Canal zone is occupied by Quaternary deposits composed of friable and loose sand sheets [18]. Quartz makes up the majority of the sand particles, with carbonate granules occasionally interfering in some areas. In terms of hydrogeology, the NWSCR is home to two aquifers: the shallow Holocene Aquifer and the deep Pleistocene Aquifer.

For the last decade, the NWSCR is suffering from several geo-environmental hazards and land degradation due to natural and human activities such as water logging, soil salinization, coastal erosion, and various types of pollution that threaten natural resources and struggle with any sustainable development planning. Therefore, this study aims to identify, delineate, and assess geo-environmental hazards that threaten NWSCR using image processing and Geographic Information System (GIS). The developed geohazard model provides decision-makers with the necessary information for development planning.

2. STUDY AREA

The Northwest Suez Canal region (NWSCR) is bordered to the north by the Mediterranean Sea, to the west by the Nile Delta, and to the east by the Suez Canal's western bank. It has a surface area of approximately 4500 km2 and is enclosed by latitudes 30° 50′ and 31° 30′ N and longitudes 31° 50′ and 32° 20′ E (Fig. 1). To the north, the NWSCR includes Manzala Lake and Port Said city, and it extends southward to El-Kantara city. The El-Salam Canal and its distributaries are located in the center of the study area, where they serve as the primary source of irrigation water for local farmers.

The NWSCR is situated east of the Nile Delta, which, like the rest of Egypt, has a hot desert climate. However, our emphasis is on the northern coast, which is the country's wettest and warmest region (with temperatures reaching 31°C) [11]. Temperatures range from 11.1°C (the coldest in January) to 30.3°C (the hottest in August). The NWSCR has an average of 9.9 rainy days per year, for a total of 83 mm of annual precipitation. The wettest month is January, with rain falling for 2.3 days and accumulating up to 18mm of precipitation. In June, July, and August, there is no rain [20]. Humidity is nearly constant throughout the year, reaching a high of 69% in December and a low of 64% in April.

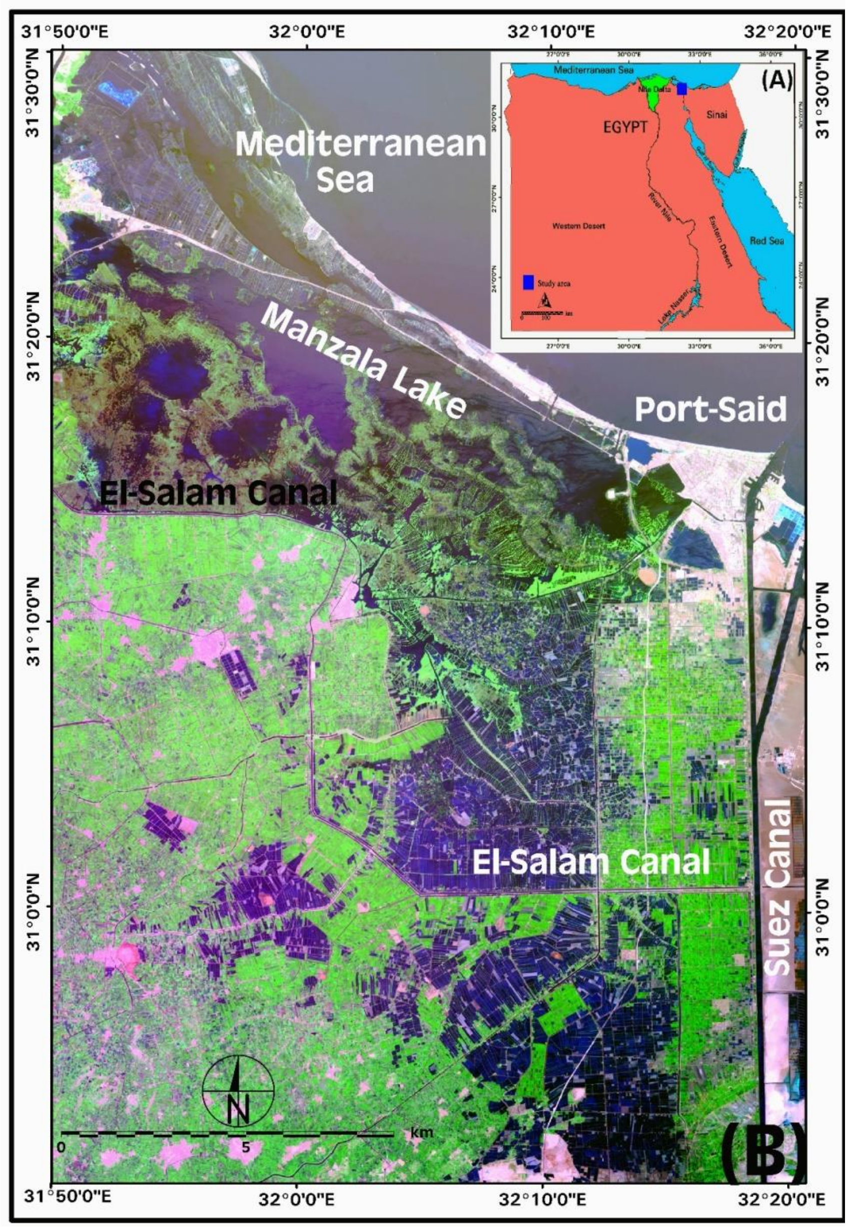

Fig (1) : A. The study area geographical location, B. The NWSCR

2.1. Regional Geology

As a portion of the Eastern Nile Delta, the NWSCR is covered in Quaternary sediments classified as Sabkha, fluviatile Nile deposits (made up of friable and loose sand sheets), and beach deposits (Fig. 2). The majority of the sand grains are quartz, with small amounts of carbonate grains found in some locations [18]. The Mediterranean Sea acts as a depositional agent in the study area, creating Pleistocene carbonate bars along the coastline zone [18]. Playa deposits form the northern boundary of Manzala Lake (Fig. 2).

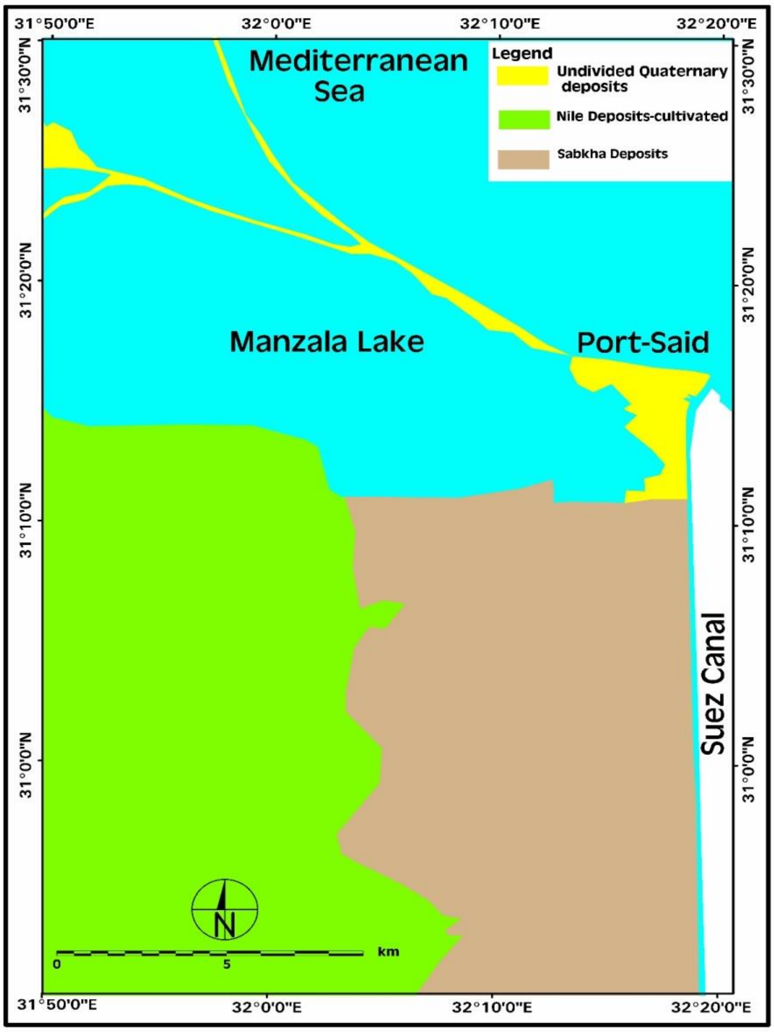

Figure 2: Lithological map of NWSCR (Modified after [28]).

Another type of deposit, such as sandy limestone, was created by Lake Manzala on its southern coast, a little northern of Ismailia [21]. The main stratum for Port Said's constructions is formed by 50 m of soft surface clay deposits on top of medium-density sand.

The Holocene deposit is formed of medium to fine-grained silt with clay in some areas and has an average thickness of 50 m close to the sea before disappearing towards the delta fringes in the south [22].

In NWSCR, Sabkhas were found on the surface. They are made of pure gypsum and clay layers, with a maximum thickness of roughly 4 m.

Beach deposits with an average thickness of around 5 m are found between Port Foad and the western side of Manzala Lake. These deposits are primarily composed of fine to medium quarzitic sand containing marine shell fragments, foraminifera, ostracods, and seaweeds[19].

2.2. Geomorphology

The NWSCR has a number of distinct geomorphologic features and a general topographic slope from south to north and northeast, with altitudes varying from 5 m above sea level to a few meters below sea level. The Eastern Lowlands are part of the Isthmus stretch, which runs from Bitter Lakes to Port Said to the north. The Nile Delta Flood Plain has a gradual slope of 1 m/km to the north with increasing thickness. The Coastal Plain encompasses the northern portion of the NWSCR. It is bounded on the north by El-Manzala Lake and extends for roughly 60 kilometers close to the current coastline. El-Manzala

Lake is the biggest lake in the Nile delta region. The Mediterranean Sea, the Damietta Branch, and the Suez Canal from its northern, western, and eastern boundaries, respectively. To connect El-Manzala Lake and the Mediterranean Sea, there is a small opening (tidal inlet) west of Port Said. The swamps crowd the Beaches of the NWSCR. The buildup of sand on beaches was caused by rising or falling sea levels. Along the coast, there are numerous marshes, ponds, and sabkhas.

3. MATERIAL AND METHODS:

In the current work, we employ the multitemporal Landsat satellite 5 and 7 images (TM and ETM+7) from the years 1984, 2000, and 2018 to examine the change in LU/LC with spatial resolutions of 30 and 15 m. Geo-rectification and correction to the WGS84 datum and the UTM N36 projection were performed on the images. The Dark-Object Subtraction method was used for atmospheric correction [23]. All image processing techniques were performed using Erdas Imagine software.

It is essential to make modifications to images to be optimized for the human visual system. Examination of digital images is the most effective way to understand the effects of near-infrared (NIR) and short-wave infrared (SWIR). The SWIR reflectance reflects variations in vegetation water content, whereas the near-infrared reflectance is altered by interior leaf structure and leaf dry matter content but not by water content. [24]By combining the NIR and SWIR, changes brought on by the amount of dry leaf matter are eliminated, and the accuracy of determining the amount of water in the vegetation is increased[24].

Principal component analysis (PCA) is common technique used in remote sensing to reduce the complexity of image data by transforming into new sets of variables, known as principal components. The global PCA is to find a linear combination of the original image bans that maximizes the variance in the data, while minimizing the correction between the new variable. The data are described with high accuracy and efficiency after applying PCA techniques. Usually, the first PCA accounts for 98% of the variance in the data set[25, 26]. A three-band PC-colored composite was shown with PC1= red, PC2= green, and PC3= blue. The three component images may be combined to form a color composite image used in the classification process and treated as original data.

The study period of 1984–2018 was separated into three sub-periods, and the LU–LC changes of the three sub-periods were compared in order to determine the change rate of LU–LC. The first period included the years 1984 through 2000, the second, 2000 through 2013, and the third, 1984 through 2018.

As a result of GIS analysis, drainage network mapping has been produced using a digital elevation model (DEM). Using a digital elevation model (DEM) as input, data are provided in two digital models, either vector layers (representing a geographic feature by the basic graphical elements of points, lines, and polygons) or raster layers (representing a geographic feature by pixels). The drainage water flow and topographic maps of the research region were both created. ArcGIS 10 was used to outline and measure waterlogged areas. Images were displayed, mosaicked, and geo-referenced using ERDAS IMAGINE 14. Along with doing image processing, augmentation, and classification by visual interpretation, (LC-LU) pattern creation is also done. All of these steps are summarized in Fig.3.

On May 18, 2021, a field survey was carried out to learn more from local farmers about the prevailing geo-environmental hazards and to validate the hazard model developed for NWSCR.

4. RESULTS AND DISCUSSION

4.1. Landuse-land cover mapping

In the current work, LC-LU maps for all classes were created for the years 1984, 2000, and 2018. These maps depict the detection of change at the NWSCR over a 34-year period. Digital image processing is used to remove digital errors and improve image quality, as well as to create thematic maps.

Several image enhancement techniques, including contrast enhancement, best band combination, image ratio, spatial filtering, and PCA, are used in this study to extract LU-LC maps to assess and monitor salinization dimension and water-logged sites at the NWSCR [25,27].

The most effective band combination for TM and ETM + was (7, 4, 2 RGB). These bands could be used to identify and demarcate the environmental features of the research area. The selection and combination of certain bands in false-color composites is based on the inter-relationship between the data enclosed in these bands. To determine the optimal combination of spectral intervals, providing the maximum information with the minimum number of intervals, is of principal importance. In remote sensing methods to identify the best results to monitor and assess the degraded areas and the environmental impact hazard indicators, the selection of optimal bands of spectral reflectance for comparison with other spectral wavelengths is required [3,12,29]. In addition, optimal digital image processing techniques are used to delineate, evaluate, and map the temporal results of remote sensing data. In the present study, the 742 RGB band combination for TM and ETM + was employed because it provides effective discrimination in geological, geomorphological, and LU-LC mapping in NWSCR. The salinized soils are white to bright white and cyan [2,20]. The color of the waterlogged area distinguishes it by various shades of blue range from dark blue to bluish-black tone or from dark blue to light blue tone. These bands can also distinguish between cultivated and urban areas (Fig. 4).

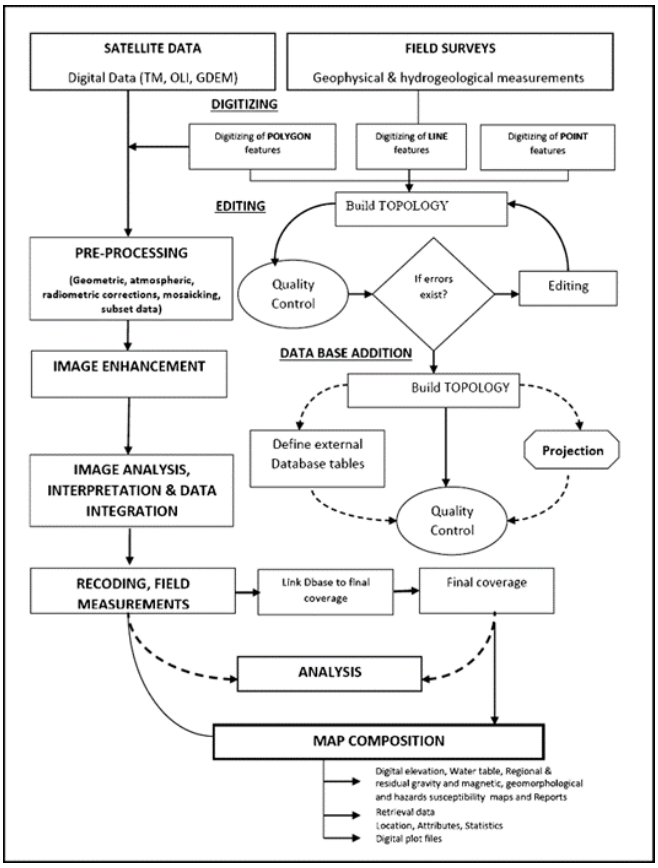

Figure 3: Flow chart summarizing the methodologies applied in the current study.

PCA analysis is used to generate images that are not correlated together in order to delineate and identify environmental hazards. PCA images of NWSCR have the highest correlation loads of PC1, PC2, and PC3, and characterize the varied LC-LU categories in the study area (Fig. 5). Based upon those findings, the salt-affected, permanent, and temporal water-logged sites and bodies are identified.

Furthermore, PCA techniques enable discrimination between urban, vegetation, saline soils, and other classes. Dark green to greenish black or greenish black to light greenish tone, as well as many hues of green, are noticeable in waterlogged zones. The color of salt-affected soils ranges from dull to bright red. The vegetation cover is distinguished by its transparent white-to-pearl color. Sabkhas zones were observed to be dull-to-bright white and cyan in color. Wetland areas can be identified by their purple color (Fig. 5).

Seven major classes can be distinguished based on the results of supervised classification (Fig.6): agricultural areas, urban areas, water bodies, fish farms, waterlogged areas, salted soil areas, and bare land areas. Furthermore, two subclasses are distinguished: industrial areas (classified as urban) and halophytic plants (classified as water bodies).

Based on the visual analysis of multi-temporal and multi-spectral Landsat imagery and field verification, the NWSCR has seen diverse environmental changes during a 34-year period. With an accuracy of 94%, the main classes of LC-LU in the research area are identified and grouped into seven classes. Agricultural areas, urban areas, water bodies and water logging zones, fish farms, halophytic plants, salted soil areas, and bare land were all included (Fig. 6).

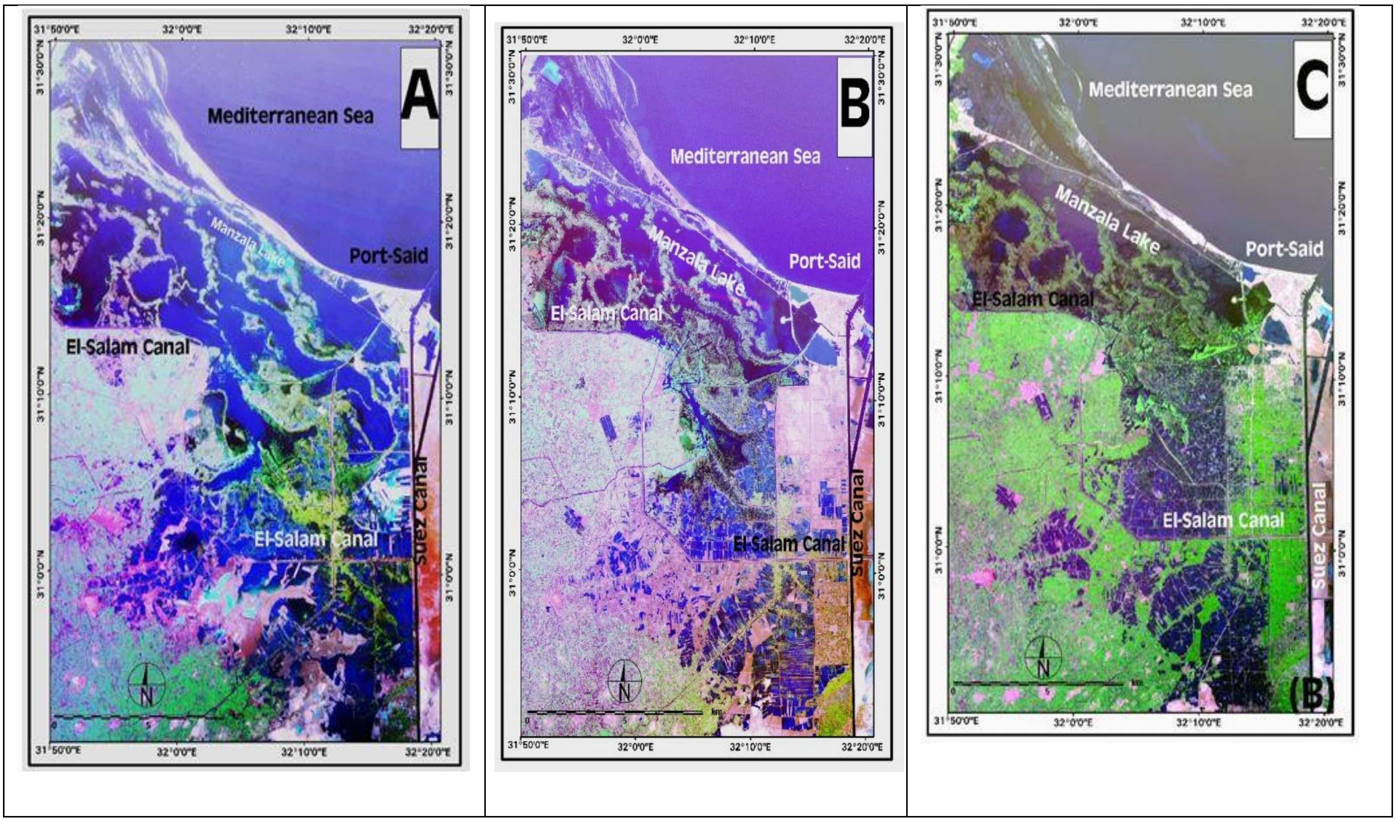

Figure (4). Best band Combinations for the multi-temporal TM, EMT+ and OLI (7, 4, 2 RGB) of NWSCR where: A:1984 B:2000 C:2018.

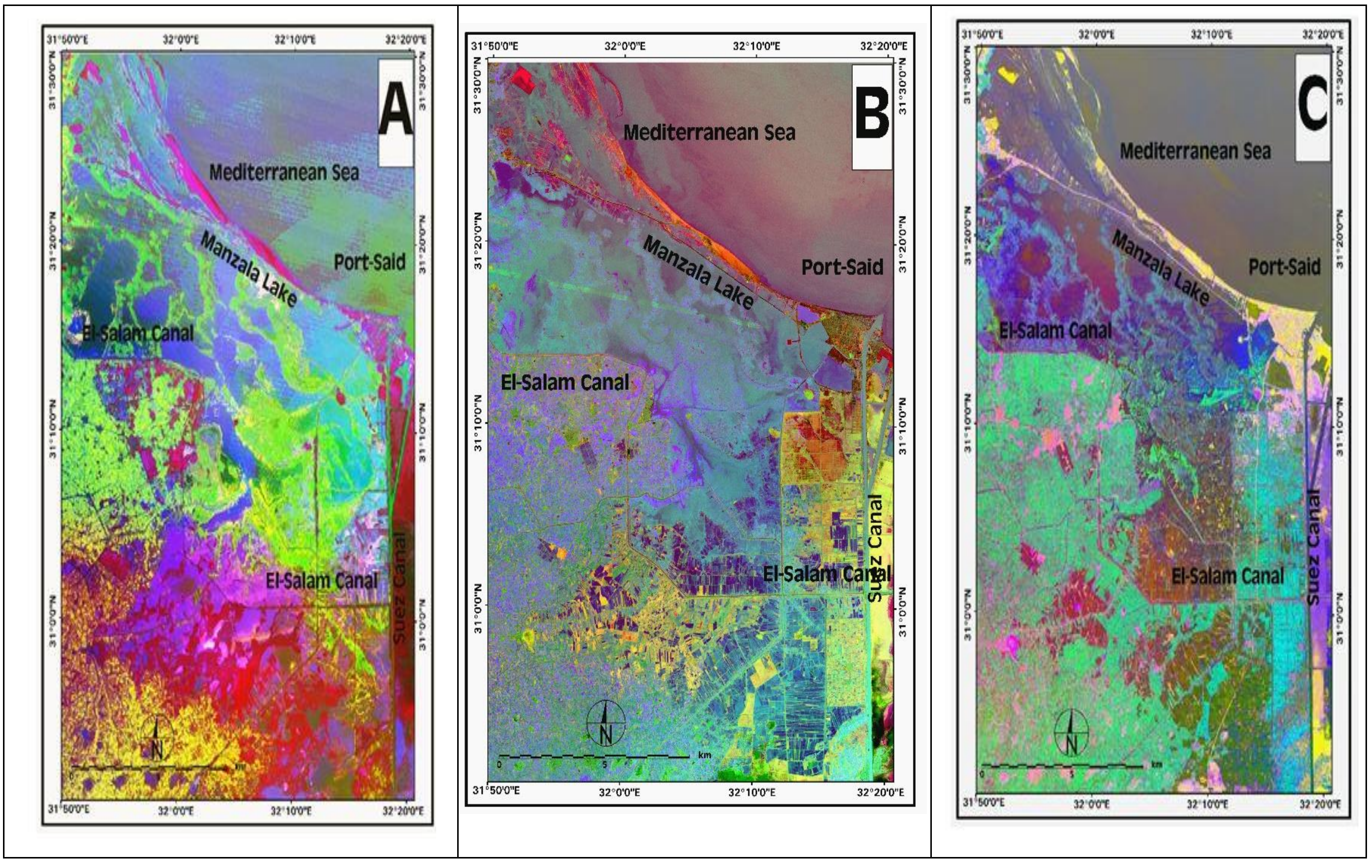

Figure 5. Enhanced PCA multi-temporal Landsat data of the PC1, PC2, and PC3 as RGB, showing the changes in the (LC-LU) classes in the NWSCR area where: A:1984 B:2000 C:2018.

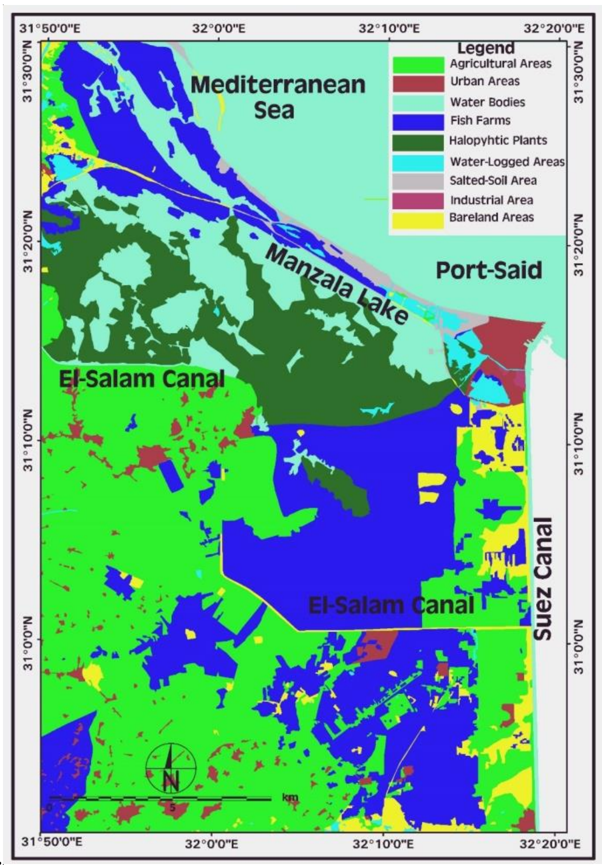

Figure 6. Supervised classification LU/LC map of NWSCR.

4.2. Detecting LC-LU changes

The NWSCR's LC-LU change detection process is categorized as having high, moderate, or low influences according to the extent of variation and deteriorated soil dangers based on these findings. LC-LU maps of the NWSCR are produced during 34-year period. They show that agricultural activity occupies around 2580.32 km^2, or 52.65% of the total area, up from 9.6% in 1984 to 40.2% in 2000. This indicates an increase in agricultural activity over the past 34 years. The water-logged areas occupy around 41.66 km^2, or 0.85% of the total area, down from 1.39% in 1984 to 1.38% in 2000. This indicates an increase in agricultural activity over the past 34 years. Unplanned urban expansion, which involves continuous new construction over LC of saline soil and bare lands, has had some salinization impacts at the NWSCR. The results in (Table 1) In this table the mathematical change detection computation of the LU/LC classes for NWSCR in 1984, 2000, and 2018.The table shows that this is evident; the urban areas in 1984 were 65.45 km^2 (2.09%), and they increased to 100.81 km^2 (2.05%) in 2018, whereas the amount of bare land decreased from 300.89 km^2 (9.53%) in 1984 to 133.28 km^2 (2.7%) in 2018.

Table 1. The mathematical change detection computation of the LU/LC classes for NWSCR in 1984, 2000, and 2018.

LU-LC Classes	1984		2000		2018	
	Area (km^2)	Percent %	Area (km^2)	Percent %	Area (km^2)	Percent %
Agricultural Areas	299.9	9.6	1793.16	40.21	2580.32	52.65
Water-logged Areas	43.6	1.39	61.58	1.38	41.66	0.85
Fish Farms	181.04	5.79	610.76	13.70	776.4	15.84
Urban Areas	65.45	2.09	69.90	1.57	99.01	2.01
Industrial areas	-	-	10.03	0.23	1.80	0.04
Water Bodies	2163.82	69.31	1424.67	31.95	1241.2	25.33
Mid. Sea	724.69	23.22	707.56	15.87	730.52	14.91
Manzala Lake	1439.13	46.10	717.11	16.08	510.68	10.42
Halophytic Plants	393.60	5.93	378.21	7.82	329.86	6.31
Salted Areas	66.81	2.14	68.25	1.53	26.33	0.53
Bare land Areas	300.89	9.63	420.47	9.43	133.28	2.71

The NWSCR also demonstrates a gradual rise in the activity of fish farms, which peaked in 2018 at 15.84% (766.4 km^2) after beginning at 5.79% (181.04 km^2) in 1984. These findings indicate that high human activities have a significant negative influence on the ecosystem. Water bodies in 1984 were 2163 km^2 (69%) and decreased to 1241.2 km^2 (25%) in 2018 as a result of Manzala lake shrinkage, which occurred over the years as a result of continuous backfilling of Manzala water body. The conducting of new agricultural projects, especially after digging El-Salam Canal and population growth is another reason for water body dimension. Because of this, the vegetation cover and appearance of urban zones have remarkably increased. The water bodies shrank from 1.3% in 1984 to 0.85% in 2018. In the NWSCR, these changes are classed as high-impact hazards induced by continuous human activity, particularly agricultural activities, and urbanization. The main causes of these consequences are agricultural activities such as flood irrigation practices and vast random land reclamation. The findings reveal an increase in human activities (mainly agricultural and urbanization) in the NWSCR over 34-year period. As a result, land reclamation and future settlement extensions at NSCWR are likely to encompass large amounts of bare and saline soils (Fig. 7).

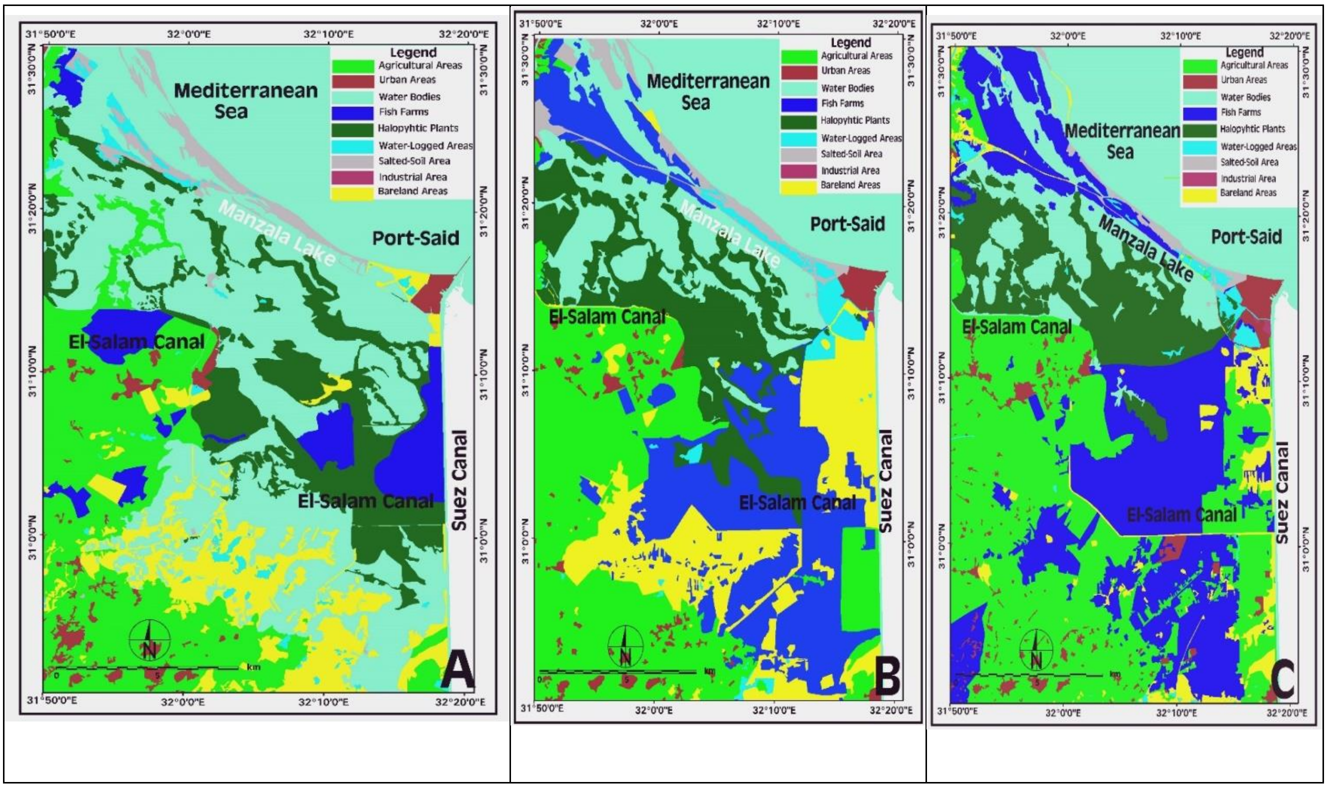

Figure 7. LC-LU maps over 34 years, displaying changes for specific categories inside the NWSCR where: A:1984 B:2000 C: 2018.

4.3. Geo-environmental hazards assessment

According to the interpretation of RS-enhanced images and field verification ((Fig. 8), the NWSCR suffered from two major land degradations: waterlogging and soil salinization. These concerns have a significant impact on soil fertility, which is reflected in soil productivity (Fig.8 field photos).

The water logging zones at the NWSCR area were divided into permanent water and temporary water logging in addition to the sensitive area for waterlogging. Permanent water logging zones are continuing all over the year. However, temporary water logging zones ended with the harvesting season in the middle of April. During May, there is an increase in the evaporations rate and agricultural activities, which increases secondary salinization. The sensitive waterlogged spots are those that appear and vanish from time to time. The obtained RS data in the NWSCR shows that 1241 km^2 of the area is permanently water-logged, 41.66 km^2 is influenced by temporary waterlogged areas, and 26.32 km^2 is influenced by saline soil.

The result of the statistics of detection of change technique for the optimized images of the entire region throughout the years 2018, 2000, and 1984 indicates the size and extent of changes in environmental hazards (salinization due to waterlogging). The extent of the waterlogged areas has changed as salt-affected soils have begun to form around the water bodies. Due to increasing salt precipitation, some of the soils close to water bodies were uncovered and later salted in different zones, but they were also inundated. These zones depict the change detection maps and wasteland conditions over the course of 34 years.

The NWSCR is dominated by four primary human activities. These were urbanization activities such as new communities, massive land reclamation, fish farming, and industrial activity. Because of these human activities, the vegetation cover in bare land areas has diminished (Table 1). The salted areas have also been removed to make way for urban areas and fish farms, which have grown dramatically in recent years due to the interest in the public in this industry.

The shrinking of Manzala Lake, which has been scarped in recent years, caused a reduction in the water bodies in 2018 as well. The "Halophytic plants" Subclass will become less common due to current scraping techniques (Fig. 9 and Table 1)

Water logging in the NWSCR is caused by canal seepage, a defective drainage network, and inefficient irrigation methods as a result of flood irrigation being the primary method of irrigation in the NWSCR. Irrigation water that percolates through the soil profile contains the majority of the salts that are still present after the evaporation and transpiration processes. Water may dissolve additional salts as it passes through the soil profile. Additionally, some salts might precipitate in the soil while others might interact with the salts in the farm's water supply. As a result, over-irrigation degrades groundwater quality.

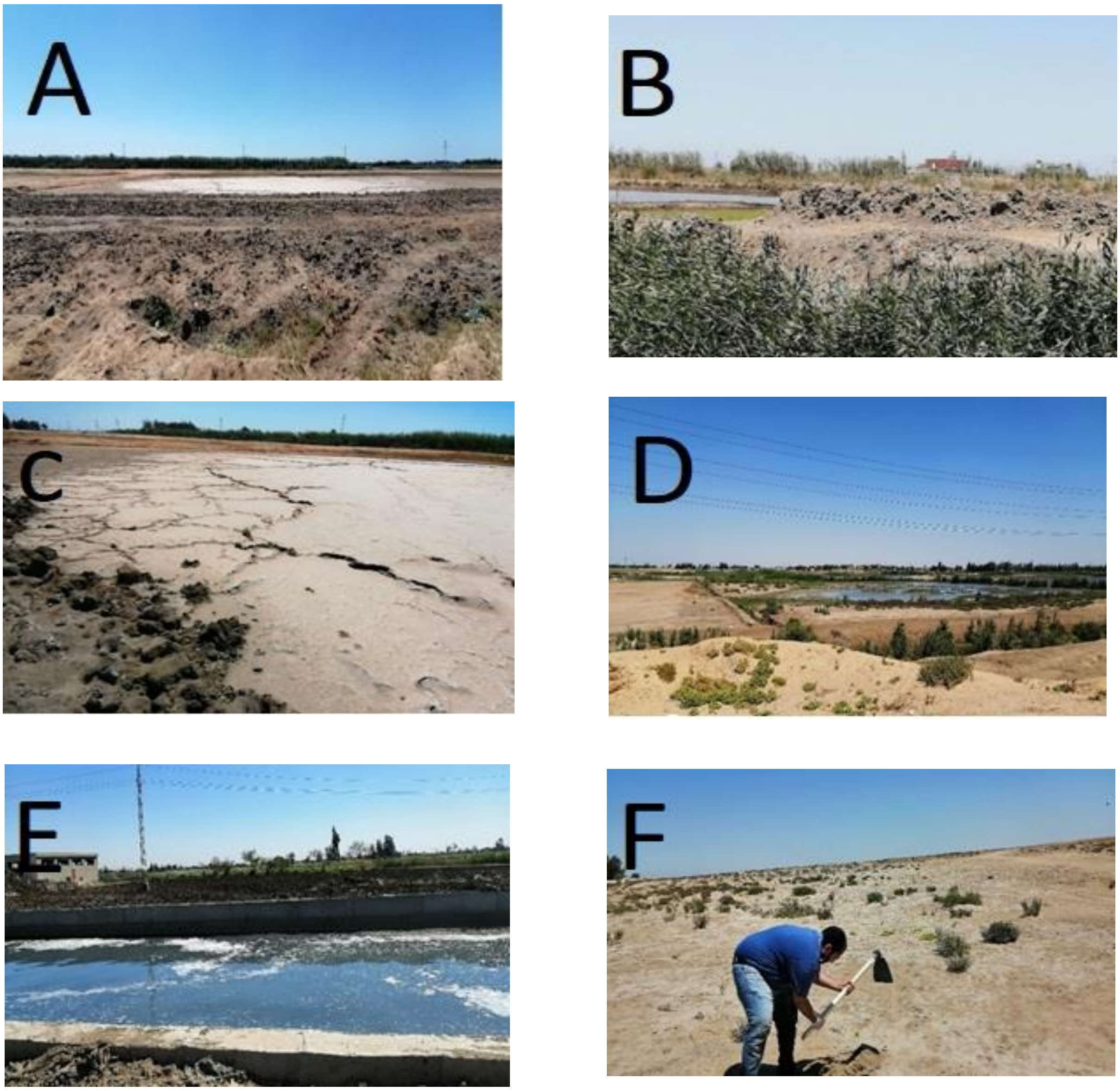

Figure 8. Field verification of environmental impact hazards at NWSCR A & C Showing Soil Salinization, B &D Showing water logging features off land degradation E show water contamination, finally F shows land desertification.

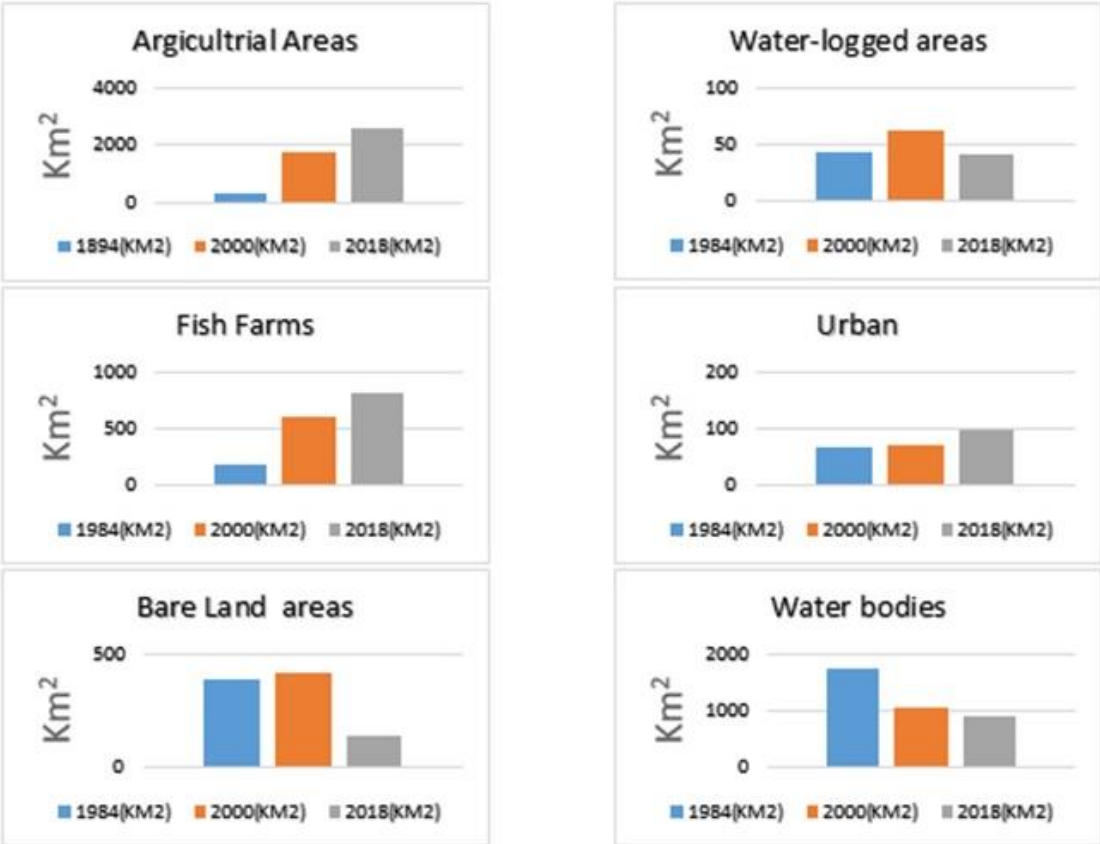

Figure 9. Charts display the evolution of the different classes of the NWSCR throughout time.

5. CONCLUSION

In the current work, an effort has been prepared to study the changes of LU/LC of NWSCR area. The best appropriate clarifications to create the optimal results for monitoring, assessing understanding and spatial mapping the LU/LC classes were achieved by employing the different image processing of available multi-temporal satellite data. The combination of RS, GIS tools, and a change detection methodology was successful in locating, mapping, and monitoring the LU-LC classes at NWSCR. Over the past few years, there has been a significant correlation between human, agricultural, and industrial activities and these land degradation aspects. The NWSCR is witnessing an increase in agricultural, urbanization and fish farm activities the water bodies and bare land classes are significantly decreased among the 1984 to 2018. The findings indicate that 1241 km^2 of the NWSCR is permanently waterlogged, 41.66 km^2 is influenced by temporary water-logged areas, and 26.32 km^2 is influenced by soil salinization. Furthermore, these findings indicate that high human activities have a significant negative influence on the ecosystem. Water bodies in 1984 were 2163 km^2 (69%) and decreased to 1241.2 km^2 (25%) in 2018 as a result of Manzala lake shrinkage, which occurred over the years as a result of continuous backfilling of Manzala water body. The present study recommends to use the modern irrigation methods to prevent the development of waterlogging and soil salinization.

6. REFERENCES

[1] Arnous M. O., El-Rayes AE, Green DR "Hydrosalinity and environmental land degradation assessment of the East Nile Delta region," Egypt. *J Coast Conserv* 19: 491–513, 2015.

[2] El-Rayes A. E., Arnous M.O., and Aziz A. "M. Morphotectonic controls of groundwater flow regime and relating environmental impacts in Northwest Sinai, Egypt, ". Arab J Geosci, 10:401, DOI 10.1007/s12517-017-3188, 2017.

[3] Arnous M.O., Mansour B. M. " Utilizing Multi-Temporal Thermal Data To Assess Environmental Land Degradation Impacts: Example From Suez Canal Region, Egypt, ". Environmental Science and Pollution Research, 30: 2145–2163, DOI: 10.1007/s11356-022-22237-z, 2023.

[4] EL-Rayes A. E., Arnous M. O., Aboulela H. A. "Hydrogeochemical and seismological exploration for geothermal resources in South Sinai, Egypt utilizing GIS and remote sensing," Arab J Geosci, 8 (8): 5631–5647, DOI 10.1007/s12517-014-1667-5.,2015.

[5] El-Rayes A. E., and Arnous M. O. " A novel approach in hydrogeochemical exploration for uranium mineralization: example from west central Sinai, Egypt," Acta Geologica Sinica (English Edition), 89 (6): 1895–1913,DOI:10.1111/1755-6724.12606,2015.

[6] Arnous M.O., El-Mowafy A. A., Azzaz S. A., Omar A. E., Abdel Hafeez, W. M. "Exploration radioactive mineralization using mappable data integration approach: example from Wadi Dahab area, Southeastern Sinai," Egypt.ArabianJournalofGeosciences,14,599.DOI:10.1007/s12517-021-06781-5,2021.

[7] Arnous M. O., El-Rayes A. E., Geriesh M. H., Ghodeif, K. O. and Al-Oshari, F. "Groundwater potentiality mapping of tertiary volcanic aquifer in IBB basin, Yemen by using remote sensing and GIS tools, " J Coast Conserv, 24,27. DOI:10.1007/s11852-020-00744-w,2020.

[8] Moubarak A. H. Arnous M. O. El-Rayes, A. E. " Integrated Geoenvironmental and Geotechnical Risk Assessment of East Port Said Region, Egypt for Regional Development, " Geotechnical and Geological Engineering, 39 (2), 1497-1520, DOI: 10.1007/s10706-020-01571-4,2021.

[9] Omran A., Fahmida K., Schröder D., Arnous M. O., El-Rayes A. E., Hochschild, V. "GIS-based rockfall hazard zones modeling along the coastal Gulf of Aqaba Region, Egypt," Earth Science Informatics, 14 (2), 691-709, DOI:10.1007/s12145-021-00580-y,2021.

[10] Arnous M.O., El-Rayes A. E., El-Nady H., Helmy, A. M. "Flash flooding hazard assessment, modeling, and management in the coastal zone of Ras Ghareb City", Gulf of Suez, Egypt. Journal of Coastal Conservation, 26 (77): 1-31, DOI: 10.1007/s11852-022-00916-w, (2022).

[11] Arnous, M.O., El-Rayes, A.E. and Helmy, A.M. (2017): Land-use / land-cover change: A key to understanding land degradation and relating environmental impacts in Northwestern Sinai, Egypt. Environmental Earth Sciences, 76(7), 26, DOI 10.1007/s12665-017-6571-3.

[12] Arnous M. O. and Green D. R. "Monitoring and assessing waterlogged and salt-affected areas in the Eastern Nile Delta region, Egypt, using remotely sensed multi-temporal data and GIS", J Coast Conserv, 19 (3): 369-391, DOI 10.1007/s11852-015-0397-5,2015.

[13] Arnous M.O. "Groundwater potentiality mapping of hard-rock terrain in arid regions using geospatial modelling: example from Wadi Feiran basin, South Sinai, Egypt" Hydrogeology Journal, 24(6):1375-1392, DOI 10.1007/s10040-016-1417-8, (2016).

[14] Arnous M. O. and El-Rayes A. E. "An integrated GIS and hydrochemical approach to assess groundwater contamination in West Ismailia area" Egypt, Arab J Geosci., Volume 6, Issue 8, pp. 2829-2842, DOI 10.1007/s12517-012-0555-0, (2013).

[15] El Raey M. ,"Vulnerability Assessment of the Coastal Zone of the Nile Delta of Egypt, to the Impacts of Sea Level Rise," *Ocean & Coastal Management*, 1997, 37: 29–40.

[16] Mabrouk M., Jonoski A., Oude Essink GHP, et al. , " Assessing the Fresh–Saline Groundwater Distribution in the Nile Delta Aquifer Using a 3D Variable-Density Groundwater Flow Model,"*Water* 11: 1946,2019.

[17] Geriesh M. H., Balke K-D, El-Rayes A. E., et al. , "Implications of climate change on the groundwater flow regime and geochemistry of the Nile Delta, Egypt," *J Coast Conserv* 19,(2015): 589–608.

[18] ELSHAZLY. E., ABDEL-HADY M., ELSHAZLY M., et al, "Geological and groundwater potential studies of El Ismailiya master plan study area," (1975).

[19] Zaki A. , "The Climatology of Nile Delta, Egypt, International Center for Agricultural Research in the Dry Areas (ICARDA) ," (2017).

[20] Aladin Weather Atlas, Port Said, Egypt - Climate & Monthly weather forecast. Available from: https://www.weather-atlas.com/en/egypt/port-said-climate.

[21] Smith NA, Welch DE, Tunbridge LW , "Investigation of the Properties of Recent Nile Delta Deposits, Port Said, Egypt ," *Geological Society, London, Engineering Geology Special Publications,* (1986), 2: 391–397.

[22] Stanley J-D, Clemente PL. I,, "ncreased land subsidence and sea-level rise are submerging Egypt's Nile Delta coastal margin,"*GSA Today*, (2017),27: 4–11.

[23] Gao B , " NDWI—A normalized difference water index for remote sensing of vegetation liquid water from space," *Remote Sensing of Environment*, (1996), 58: 257–266.

[24] Ceccato P, Flasse S, Grégoire J-M , "Designing a spectral index to estimate vegetation water content from remote sensing data: Part 2. Validation and applications," *Remote Sensing of Environment*, (2002), 82: 198–207.

[25] Jensen JR. , "Introductory digital image processing: a remote sensing perspective," Prentice-Hall Inc, (1996).

[26] Gibson P, Gibson PJ, Power C, et al. , "Introductory remote sensing: Digital image processing and applications," (2000),Psychology Press.

[27] Lillesand TM, Kiefer RW, Chipman J , " Remote sensing and image analysis," *Joh n Wiley and Sons, New York, NY, USA*(2000).

[28] EGSM "GEOLOGIC MAP OF EGYPT 1981" Ministry of Industry and Mineral Resources, the Egyptian Geological Survey and Mining Authority 1981.

[29] Ghodeif, K O, Arnous, M O Geriesh, M H, " Define a protected buffer zone for Ismailia Canal, Egypt using Geographic Information Systems, " Arab J Geosci, Volume 6, Issue 1, pp. 43-53, DOI 10.1007/s12517-011-0326-3(2013).